Biosystems Engineering (2002) **82** (2), 199–207
doi:10.1006/bioe.2002.0072, available online at http://www.idealibrary.com on IDEAL®
SE—Structures and Environment

Scale Model Analysis of Opening Effectiveness for Wind-induced Natural Ventilation Openings

Hsin Yu[1]; Chiu-Hsiung Hou[2]; Chung-Min Liao[2]

[1]Department of Civil Engineering, National Ilan Institute of Technology, Ilan 260, Taiwan, ROC; e-mail: yuhsin@mail.ilantech.edu.tw
[2]Department of Bioenvironmental Systems Engineering, National Taiwan University, Taipei 10617, Taiwan, ROC; e-mail of corresponding author: cmliao@ccms.ntu.edu.tw

(Received 17 April 2001; accepted in revised form 6 March 2002; published online 11 June 2002)

An algorithm is developed to predict the opening effectiveness for wind-induced natural ventilation openings. The method is based on distorted scaling theory with the Buckingham Pi theorem to determine the relationship among the non-dimensional parameters. The non-dimensional parameters chosen were Reynolds number, wind angle of incidence, ratio of height to length of opening and roof slope. Model validation was conducted in a wind tunnel using scale models under isothermal conditions. Types of sidewall opening and covered ridge with sidewall opening for natural ventilation systems in the Taiwan region were employed to compare the opening effectiveness. During the experiments, wind angle of incidence varied from 10 to 90°, wind velocity varied from 1·5 to 4·5 m s^{-1}, roof slope varied from 10 to 30°, and ratio of height to length of opening varied from 1/3 to 1. Wind speed and wind angle of incidence were the dominant factors determining opening effectiveness in both types. The covered ridge with sidewall opening proved more effective than the sidewall opening type. This work provides practical information to improve the quality control of microclimate in wind-induced naturally ventilated enclosures.

1. Introduction

Natural ventilation is widely used in hot and warm climates with the advantages of saving energy, expense and installation time. Greenhouses, livestock buildings, and dwelling houses are controlled by natural convection to remove excessive heat and moisture. The mechanism of natural ventilation depends on wind effects, thermal buoyancy and the combination of both wind and buoyancy forces. Thermal buoyancy is less important than the wind effect for natural ventilation, especially in hot weather (ASHRAE, 1997; Barrington *et al.*, 1994). Wind speed and wind direction are the dominant factors for wind-induced effects. de Jong and Bot (1992), Verlinde *et al.* (1998) and Miguel *et al.* (2001) indicated that a full understanding of the relationship between wind characteristics (wind speed and wind direction) and ventilation characteristics (dimensions, inlet and outlet design, *etc.*) are required to achieve sufficient natural ventilation.

Natural ventilation openings include (i) windows, doors, monitor openings, and skylights; (ii) roof ventilators; (iii) stacks connecting to registers and (iv) special designed inlet or outlet openings (ASHRAE, 1997). The most popular types of natural ventilation openings employed in Taiwan region are windows, doors, roof ventilators (open ridge ventilation) and roof ventilators with a raised roof section (covered ridge ventilation) The characteristics of openings affect natural ventilation efficiency with the arrangement, location, and control of ventilation openings to achieve a desired ventilation rate and good distribution of ventilation air through the buildings (ASHRAE, 1997; de Zwart & Bot, 1997; Miguel *et al.*, 1998). Albright (1990) also recommended the roof slopes not less than 1:4 to promote ventilation by thermal buoyancy during cold weather with little wind.

The natural ventilation rate depends on the effect of wind moving through openings. ASHRAE (1997) suggests an empirical expression to predict the flow through a sidewall opening as a function of wind speed and opening effectiveness as

$$Q = EAV \tag{1}$$

Notation

A	area of inlet opening, m^2	V	wind velocity, $m\,s^{-1}$
E	opening effectiveness	α	distortion factor
f	function of parameters	δ	prediction factor
H	height of opening, m	θ	roof slope
k, k_n	constant coefficient	π	dimensionless parameter
L	length of opening, m	ρ	air density, $kg\,m^{-3}$
m	number of basic independent dimensional units	μ	absolute air viscosity, $N\,s\,m^{-2}$
m_r	actual mass flow rate, $kg\,s^{-1}$	ϕ	wind angle of incidence
m_t	theoretical mass flow rate, $kg\,s^{-1}$		
n	number of independent variables	*Subscripts*	
n_n	constant exponent	a, b	Specific value
Q	airflow rate, $m^3\,s^{-1}$	m	model
Re	Reynolds number ($\rho Vl/\mu$)	p	prototype
V_r	actual air velocity, $m\,s^{-1}$	r	real
V_t	theoretical air velocity or wind speed, $m\,s^{-1}$	t	theoretical

where Q is the airflow rate in $m^3\,s^{-1}$, E is the opening effectiveness (dimensionless), A is the area of inlet opening in m^2, and V is the wind velocity in $m\,s^{-1}$.

ASHRAE (1997), Albright (1990), Esmay and Dixon (1986) and Hellickson *et al.* (1983) recommended that the values of E were 0·50–0·60 for perpendicular wind and 0·25 to 0·35 for diagonal wind. A value of 0·35 is normally employed for agricultural buildings.

Nääs *et al.* (1998) developed an empirical algorithm to predict the opening effectiveness of naturally ventilated buildings. The parameters of the equation include roof slope, wind angle of incidence, ratio of height to length of opening and Reynolds number in the range of turbulent airflow. Results from Nääs *et al.* (1998) indicated that the wind direction and wind velocity are the most influential factors of opening effectiveness.

Verlinde *et al.* (1998) also developed a similar algorithm and concluded that the parameters affecting the opening effectiveness are wind speed, roughness of the surrounding field, wind angle of incidence, windscreens of the inlet opening and spoilers on the roof. Their experimental results showed that the wind angle of incidence is the most significant parameter and the roughness of the surrounding fields has only little influence on opening effectiveness.

The purpose of this study is to find the quantitative expressions of opening effectiveness for wind-induced natural ventilation for two types of openings, one with sidewall openings and the other with covered ridge and sidewall openings that are commonly employed in the Taiwan region. A wind tunnel technique was developed to quantify scale model performance under controlled conditions and to extend the range of scale models analysed.

2. Theoretical considerations

Generally, the known scaling laws are used to represent the flow between scale model and prototype. The results of scale model analysis can be used to predict the flow behaviour in a prototype based on the similitude criteria.

The traditional Buckingham Pi (π) theorem (Murphy, 1950) is commonly used to derive an empirical relationship between opening effectiveness and variables in terms of dimensionless parameters. The method develops n–m dimensionless π terms, where n independent variables are related to the problem using m basic independent dimensional units. Each π can be described by a function of the other dimensionless parameters in the following expression:

$$\pi_1 = f(\pi_2, \pi_3, \pi_4, \pi_5) \tag{2}$$

Equation (2) indicates that only knowledge of the variables related to the problem of interest is required. Young (1994) pointed out that, with this method, if one or more important variables are neglected, serious mistakes of model design can result.

A systematic procedure for studying the function between π terms is to vary specific parameters while holding others constant (Murphy, 1950; Young, 1994). These component equations can be described as the following forms if the π terms are formed in a logarithmic space:

$$(\pi_1)_2 = f(\pi_2, \bar{\pi}_3, \bar{\pi}_4, \bar{\pi}_5) = k_2\pi_2^{n_2} \tag{3}$$

$$(\pi_1)_3 = f(\bar{\pi}_2, \pi_3, \bar{\pi}_4, \bar{\pi}_5) = k_3\pi_3^{n_3} \tag{4}$$

$$(\pi_1)_4 = f(\bar{\pi}_2, \bar{\pi}_3, \pi_4, \bar{\pi}_5) = k_4\pi_4^{n_4} \tag{5}$$

$$(\pi_1)_5 = f(\bar{\pi}_2, \bar{\pi}_3, \bar{\pi}_4, \pi_5) = k_5\pi_5^{n_5} \tag{6}$$

where k_{2-5} are coefficients and n_{2-5} are exponents, the bar above symbols denoting a constant value. The general equation is given by the following form:

$$\pi_1 = \frac{f(\pi_2, \bar{\pi}_3, \bar{\pi}_4, \bar{\pi}_5) f(\bar{\pi}_2, \pi_3, \bar{\pi}_4, \bar{\pi}_5) f(\bar{\pi}_2, \bar{\pi}_3, \pi_4, \bar{\pi}_5) f(\bar{\pi}_2, \bar{\pi}_3, \bar{\pi}_4, \pi_5)}{f(\bar{\pi}_2, \bar{\pi}_3, \bar{\pi}_4, \bar{\pi}_5)^{5-2}} \tag{7}$$

and every $\bar{\pi}_n$ must be the same in each set. Substituting the components in Eqns (3) to (6) into Eqn (7) results in

$$\pi_1 = k\pi_2^{n_2}\pi_3^{n_3}\pi_4^{n_4}\pi_5^{n_5} \tag{8}$$

where the coefficient k is given by

$$k = \frac{k_2 k_3 k_4 k_5}{f(\bar{\pi}_2, \bar{\pi}_3, \bar{\pi}_4, \bar{\pi}_5)^3} \tag{9}$$

True models (subscript m) are defined as satisfying all required design conditions of the prototype (subscript p)

$$\begin{aligned} (\pi_1)_p &= (\pi_1)_m \\ (\pi_2)_p &= (\pi_2)_m \\ (\pi_3)_p &= (\pi_3)_m \\ (\pi_4)_p &= (\pi_4)_m \\ (\pi_5)_p &= (\pi_5)_m \end{aligned} \tag{10}$$

If one or more design conditions of scale model are not satisfied, then the models are defined as distorted models. A prediction factor δ should be added to correct the resultant parameter of scale model as

$$(\pi_1)_p = \delta(\pi_1)_m \tag{11}$$

If the distortion factor α exists in a specific π term, say π_3, as

$$(\pi_3)_p = \left(\frac{1}{\alpha}\right)(\pi_3)_m \tag{12}$$

then the relationship between δ and α is

$$\delta = \left(\frac{1}{\alpha}\right)^{n_3} \tag{13}$$

The general equation of π_1 in distorted models becomes

$$\pi_1 = \delta f(\pi_2, \pi_3, \pi_4, \pi_5) \tag{14}$$

or

$$\pi_1 = k\pi_2^{n_2}\left(\frac{\pi_3}{\alpha}\right)^{n_3}\pi_4^{n_4}\pi_5^{n_5} \tag{15}$$

The dimensionless parameters selected in the present study include: (i) the Reynolds number defined by the opening length, air density, air velocity, and absolute air viscosity; (ii) the ratio between opening height and opening length; (iii) the incidence angle of wind flow and (iv) the slope of roof. These dimensionless parameters were used to develop the model of opening effectiveness as in the following expression:

$$E = k(0{\cdot}2\,\mathrm{Re})^{n_2}\left(4\frac{h}{l}\right)^{n_3}(\sin\phi)^{n_4}(\sin\theta)^{n_5} \tag{16}$$

where Re is the Reynolds number ($\mathrm{Re} = \rho V l/\mu$, in which ρ is the air density in $\mathrm{kg\,m^{-3}}$, V is the air velocity in $\mathrm{m\,s^{-1}}$, $\mu$is the absolute air viscosity in $\mathrm{Ns\,m^{-2}}$, and l is the opening length in cm); h/l is the ratio of opening height to opening length; ϕ is the wind flow angle of incidence and θ is the roof slope angle.

The height and length of the scale model are distorted by a factor of 5 and 20, respectively, resulting in the calibrated factors of 0.2 [= (20/5)/20] and 4 (= 20/5) in Eqn (16). The functional relations between the π terms were determined experimentally (Shepherd, 1965; Fox & McDonald, 1973; Nääs *et al.*, 1998). All parameters were maintained fixed when experiments proceeded in a wind tunnel except for the parameter of interest to determine the coefficients of expression of opening effectiveness. To find the coefficient of Reynolds numbers, for example, wind velocity was measured when all other parameters maintained constant.

Two specific values (denoted by subscript a and b) for the opening effectiveness were determined as

$$E_a = k(0{\cdot}2\frac{\rho V_a l}{\mu})^{n_2}(4\frac{h}{l})^{n_3}(\sin\phi)^{n_4}(\sin\theta)^{n_5} \tag{17}$$

$$E_b = k(0.2\frac{\rho V_b l}{\mu})^{n_2}(4\frac{h}{l})^{n_3}(\sin\phi)^{n_4}(\sin\theta)^{n_5} \tag{18}$$

then

$$E_a/E_b = \left(V_a/V_b\right)^{n_2} \tag{19}$$

or

$$n_2 = \ln\left(E_a/E_b\right)/\ln\left(V_a/V_b\right) \tag{20}$$

This procedure was applied for other parameters and obtained as

$$n_3 = \ln\left(E_a/E_b\right)/\ln\left[\left(h_a/l_a\right)/\left(h_b/l_b\right)\right] \tag{21}$$

$$n_4 = \ln\left(E_a/E_b\right)/\ln\left[\sin\phi_a/\sin\phi_b\right] \tag{22}$$

$$n_5 = \ln\left(E_a/E_b\right)/\ln\left[\sin\theta_a/\sin\theta_b\right] \tag{23}$$

The value of the opening effectiveness is defined as the ratio of mass of air that flows through openings to the theoretical mass of air that entered such that

$$E = m_r/m_t = (\rho V_r A)/(\rho V_t A) \tag{24}$$

where m_r is the actual mass flow rate in $\mathrm{kg\,s^{-1}}$, m_t is the theoretical mass flow rate in $\mathrm{kg\,s^{-1}}$, V_r is the actual air velocity in $\mathrm{m\,s^{-1}}$, and V_t is the theoretical air velocity or wind speed in $\mathrm{m\,s^{-1}}$. For constant air density

$$E = \left(\Sigma V_r/\Sigma V_t\right) \tag{25}$$

that represents the opening effectiveness deriving from wind tunnel experiments.

3. Materials and methods

3.1. *Wind tunnel system*

An open, compact, low-speed, temperature and humidity controlled wind tunnel system was used to simulate the wind-induced natural ventilation through a modelled enclosure under steady-state condition in laboratory. The design criteria represented an air speed of $< 10\,m\,s^{-1}$, temperature under 50°C, relative humidity of 10–95%, and a spatially uniform and steady free air stream in the portion of the test section.

The wind tunnel (*Fig. 1*) used for the model study was divided into three sections: a rectifying contraction section, a test/measurement section, and an air duct section (Liao & Chiu, 2002).

The rectifying contraction section was 70 cm long and made in Plexiglas for easy viewing. A fibreglass honeycomb baffle (*i.e.* an anti-turbulence screen) was constructed at the entrance of the rectifying contraction section (60 cm by 60 cm) to ensure constant and uniform inlet air distribution. Turbulent airflow created by intake air was minimized in the front part of the section. The extended area was narrowed down to 30 cm by 30 cm by a contraction-cone-profile design to keep the stream evenly distributed.

The test/measurement section offered a cross-sectional area of 30 cm by 30 cm along a length of 90 cm. This section contained the instrumentation for temperature, air velocity, and pressure differences between static and total pressure in a space front of the opening or inside the scale model.

An air duct section made of a circular metal duct with a profile design (52 cm in length and 30 cm in diameter for the inlet opening, then narrowing down to 22 cm in diameter) was attached to the end of test section. A 170 cm long plastic-flexible circular duct of 30 cm in diameter was attached to the metal duct.

A centrifugal fan of 30 cm in diameter, driven by a multi-speed 0·75 kW three-phase induction electric motor (Teco. Elec. and Mech. Co., Ltd., Taiwan), controlled by a transistor inverter (Kassuga Electric Works, Ltd., Japan), induces the air through the wind tunnel. A powerful 12 A motor varying from 0 to $10\,000\,min^{-1}$ was adjusted to give a particular flow rate by a precise motor control unit. The centrifugal fan contains a rotating impeller mounted inside a scroll-type housing. The motor and intake profiles were made of fibreglass to minimize airflow distortion.

3.2. *Procedure and instrumentation*

Distorted models were constructed using 1.5 cm thick Chinese cypress to test the wind-induced natural ventilation with dimensions fitting the test section of the wind tunnel measuring the 30 cm wide by 30 cm high by 90 cm in length. The height and length of both scale models were reduced by 5 and 20 times, respectively, to accommodate the test section of wind tunnel. The sidewall openings (SP) were 20 cm wide, 18 cm high, and

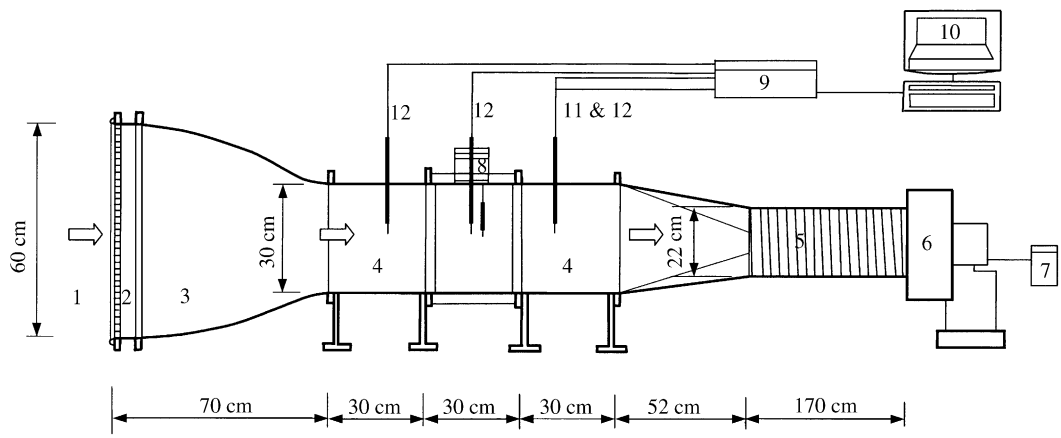

Fig. 1. A compact wind tunnel system used for the performance evaluation of opening effectiveness of wind-induced natural ventilation enclosures. (1) protection net, (2) honeycomb baffle, (3) contraction section, (4) test section, (5) air duct section; (6) fan, (7) transistor inverter, (8)anemometer, (9) CR10 micrologger, (10) personal computer, (11) thermocouples and (12) pressure transducer

20 cm long (*Fig. 2*), and flora for the covered ridge with sidewall openings (CRSP) were 20 cm wide, 27 cm high, and 20 cm long (*Fig. 3*). The joints of the scale models were tightly sealed to reduce errors in pressure measurement. The ratios of height to length of opening were 1/6–1/3 for both sidewall openings and covered ridge with sidewall openings.

The incidence angles between wind direction and the opening surface ranged from 10 to 90°. The roof slope angle varied from 10 to 30°. The laboratory temperature remained at 25 ± 1°C. An anemometer (Model 4510, Testoterm, Germany) was mounted at midpoint inside the scale model to measure the induced airspeed, and, simultaneously, the temperature inside the scale model. T-type copper-constantine thermocouples were used to measure the temperature outside the scale model.

Two pressure transducers (Model 600, Auto Tran Inc., USA) measured the pressures across the opening positioned in the front and back of the model. The frequency of pressure measurement is 6 Hz with a duration of 1 min.A data logger (Model CR10, Campbell Sci. Inc., USA) recorded all data for analysis.

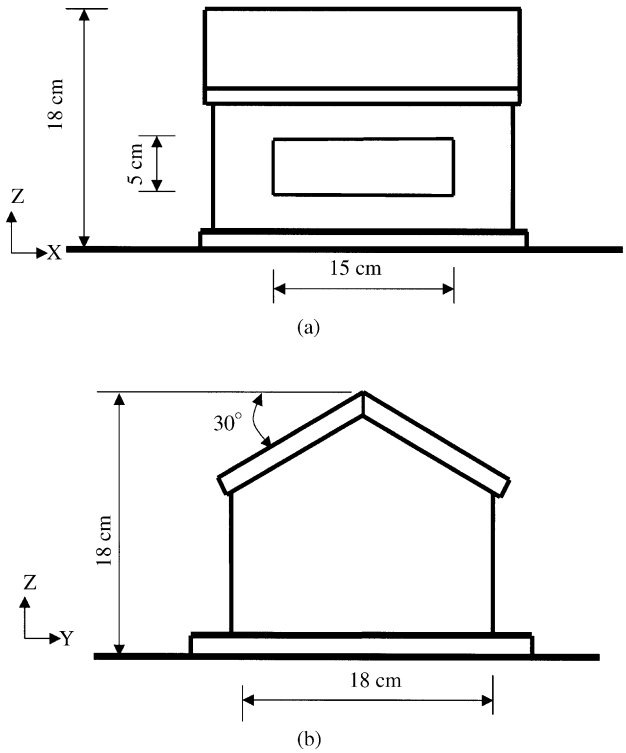

Fig. 2. Dimensions for the scale model of the sidewall opening type: (a) traverse side view and (b) longitudinal side view

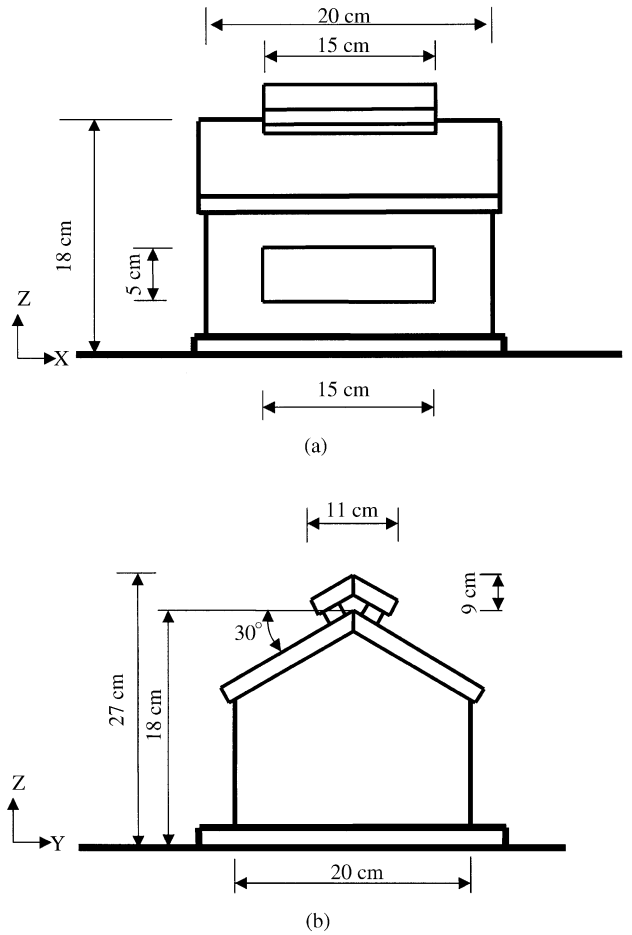

Fig. 3. Dimensions for the scale model of the covered ridge with sidewall opening type: (a) traverse side view and (b) longitudinal side view

4. Results and discussion

4.1. *Expressions of opening effectiveness*

The values of n_2 and k_2 for the sidewall openings were calculated for two wind speeds of 1·5 and 4·5 m s^{-1} and two opening effectiveness values by applying Eqns (3) and (20) and using the data in Table 1.

Table 2 lists the calculated values of the n_n and k_n for SP type openings by varying h/l, ϕ and θ. The expression of opening effectiveness for SP-type openings use consistent terminology substituting all Table 2 parameters into Eqn (16), and shows the influence on opening effectiveness of wind angle of incidence ϕ, wind speed V, ratio of height to length of opening h/l and roof slope θ.

The equation for opening effectiveness for the CRSP type can also be derived from a similar algorithm. The values n_n and k_n for a covered ridge with sidewall

Table 1
Velocity measurements used to calculate exponent n_2 and coefficient k_2 of expression of opening effectiveness for the sidewall opening (SP) type*

Height (Z) cm	*Actual velocity (V_r) m s^{-1}*	
	Wind speed (V_t) at 1·5 m s^{-1}	*Wind speed (V_t) at 4·5 m s^{-1}*
	0·90	1·80
6·5	0·90	1·80
	1·00	1·90
	1·10	2·30
9·5	1·00	2·30
	1·10	2·50
	1·20	2·60
12·5	1·10	2·40
	1·20	2·40
	0·90	1·80
15·5	1·00	1·80
	1·10	1·90
Average velocity	1·04	2·13
Standard deviation	0·11	0·32

* Temperature $T = 25°C$; roof slope, $\theta = 30°$; wind angle, $\phi = 90°$; opening height to length ratio; $h/l = 1/3$.

openings are again shown in Table 2. Substituting all the parameters of Table 2 into Eqn (16) gives the expression for the CRSP opening effectiveness.

The resultant algorithms imply that wind speed V and wind angle of incidence ϕ affect opening effectiveness significantly, whereas the ratio of height to length of opening h/l and roof slope θ are the less dominant factors. The expressions for opening effectiveness for the SP and CRSP types also increase exponentially with h/l and ϕ, yet decrease exponentially with wind speed and roof slope. The exponent of the ratio h/l term has a positive sign, while that of Nääs *et al.* (1998) was negative. Aynsley (1988) pointed out that friction losses increase with hydraulic radius of the airway (cross-sectional area/perimeter). The hydraulic radius of sidewall opening of present model is inversely proportional to the ratio of height to length of opening. The ventilation effectiveness E is inversely proportional to the frictional losses and is proportional to the ratio of height to length of opening (*Fig. 5)*.

Table 2 also demonstrates that the ventilation effectiveness E is lower with higher wind speeds. The ventilation effectiveness E is similar as the discharge coefficient that is the product of the coefficient of velocity and contraction. The discharge coefficient accounts for energy loss due to friction, turbulence, section change and other entrance effects (Hellickson *et al.*, 1983). Two types of energy loss are encountered with wind-induced ventilation through large openings in buildings, dynamic and frictional. Dynamic loss is associated with airflow through an opening, and abrupt expansion or bend is occurred in cross section of the airway, and jet energy dissipated from an outlet. Frictional loss is associated with skin friction as the viscous air moves past the surface of the airway. Frictional losses increase with surface roughness and are proportional to airflow velocity (Aynsley, 1988). Experimental results demonstrate that the ventilation effectiveness is inversely proportional to the inlet Reynolds number in airflow through hinged baffle slotted inlets (Albright, 1976), in fluid flow through orifice in pipes (Fox & McDonald 1973), and in wind through large openings (Nääs *et al.*, 1998).

4.2. *Effect of wind angle of incidence*

To derive the effect of wind angle of incidence, the experiments were conducted using a constant roof slope ($\theta = 30°$) and a constant ratio of height to length of opening ($h/l = 1/3$) for a temperature of $25 \pm 1°C$.

Table 2
Calculated coefficients of n_n and k_n for sidewall opening (SP) type and covered ridge with sidewall opening (CRSP) type

Parameters	*Opening effectiveness*		*Exponents*	*Coefficients*
	E_a	E_b	(n_n)	(k_n)
SPT type				
Wind velocity V, m s^{-1}	0·69	0·47	−0·3495	11·19
Height to length ratio h/l	0·64	0·47	0·2810	0·43
Wind angle ϕ, degree	0·15	0·56	0·7524	0·47
Roof slope angle θ, deg	0·56	0·47	−0·1657	0·42
CRSP type				
Wind velocity V, m/s	0·74	0·48	−0·3940	17·10
Height to length ratio h/l	0·65	0·48	0·2760	0·54
Wind angle ϕ, deg	0·15	0·70	0·8799	0·48
Roof slope angle θ, deg	0·63	0·48	−0·2571	0·40

Calculations show that the opening effectiveness for both types increased with increasing wind angle. The opening effectiveness was higher with lower wind speed at the same wind angle. The value of E for the SP type ranged from 0·18 to 0·69, 0·14 to 0·54 and 0·13 to 0·47 at wind speeds of 1·5, 3 and 4·5 m s^{-1}, respectively, and for wind angles of 10–90°; whereas for the CRSP type, values of E were 0·19–0·90, 0·15–0·68, 0·10–0·47 at wind speeds of 1·5, 3 and 4·5 m s^{-1}, respectively, for the same wind angles of incidence.

Figure 4 compares opening effectiveness values at specific wind speeds of 5 and 10 m s^{-1}. The opening effectiveness of the SP type is slightly larger than that of the CRSP type, for the same wind angle of incidence and wind speeds of 5 and 10 m s^{-1}. Both values of opening effectiveness are less than that of Nääs *et al.* (1998), yet close to values obtained from ASHRAE (1997), Choinere (1991), Hellickson *et al.* (1983) and Verlinde *et al.* (1998).

4.3. *Effect of ratio of height to length of opening*

Calculation results indicate that opening effectiveness increased with increasing ratio of height to length of opening by maintaining a constant roof slope ($\theta = 30°$) and wind angle of incidence ($\phi = 90°$). The opening effectiveness was higher for a lower wind speed at the same ratio of height to length of opening. The value of E for the SP type ranged from 0·69 to 0·93, 0·54 to 0·73, and 0·47 to 0·64 at wind speeds of 1·5, 3 and 4·5 m s^{-1}, respectively, for h/l ratio of 1/3 and 1; whereas the value of E for the CRSP type ranged from 0·73 to 0·99, 0·56 to 0·75, and 0·47 to 0·64 at wind speed. of 1·5, 3 and 4·5 m s^{-1}, respectively, for h/l ratios of 1/3 and 1.

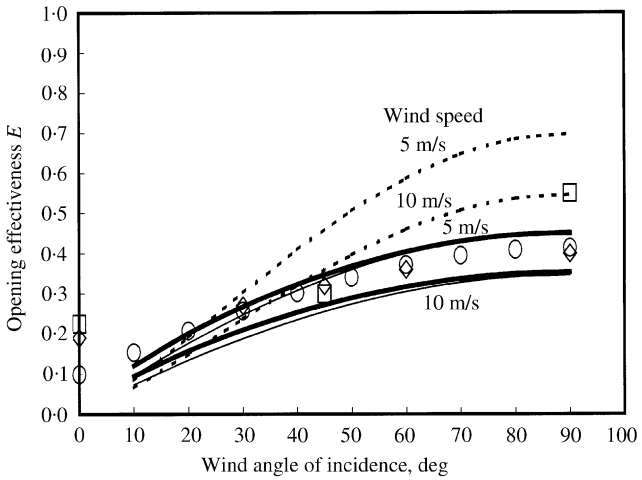

Fig. 4. Comparative opening effectiveness with variations in wind angle of incidence for roof slope angle θ = 30° and height to length ratio h/l = 1/3: ▬, sidewall opening type; ——, covered ridge with sidewall opening type; - - - -, Nääs et al. (1998); ○, Verlinde et al.(1998) at wind speeds of 2.6, 6 and 11 m s^{-1}; □, ASHRAE (1997) at normal wind speeds; ◇, Choinére (1991) at normal wind speeds

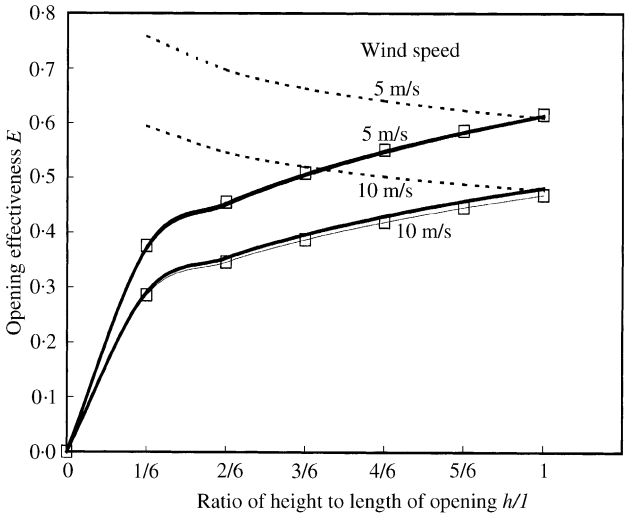

Fig. 5. Comparative opening effectiveness with variations in ratio of height to length of opening for roof slope angle θ = 30° and wind angle of incidence φ = 90°: ▬, sidewall opening type; □, covered ridge with sidewall opening type; - - - -, Nääs et al. (1998). The opening effectiveness for sidewall and covered ridge with sidewall opening types superimposes the lines at wind velocity of 5 m s^{-1}, indicating very low variation in model output as wind velocity at 5 m s^{-1}

Comparisons of opening effectiveness with different h/l ratios are shown in *Fig. 5*. The trends in opening effectiveness differ from those of Nääs *et al.* (1998). Values of opening effectiveness increased with increasing h/l. The values increased rapidly when h/l was under 1/6 for both types, suggesting that h/l should be larger than 1/6 to achieve a higher opening effectiveness.

4.4. *Effect of roof slope*

The effect of roof slope (10, 20 and 30°) was obtained under a constant wind angle of incidence ($\phi = 90°$) and ratio of height to length of opening ($h/ = 1/3$). The results show that opening effectiveness decreased slightly with increasing roof slope for the SP type. The value of E for the SP type ranged from 0·69 to 0·82, 0·54 to 0·64, and 0·67 to 0·56 at wind speeds of 1·5, 3 and 4·5 m s^{-1}, respectively, with roof slopes of 10–30°. The opening effectiveness E did not vary significantly with roof slope for the SP type. Results also show that opening effectiveness decreased with increasing roof slope for

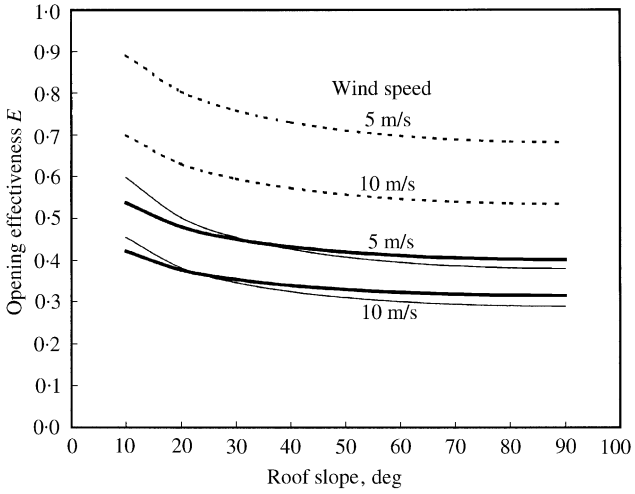

Fig. 6. Comparative opening effectiveness with variations in roof slope angle for ratio of height to length of opening h/l = 1/3 and wind angle of incidence $\phi = 90°$: ▬, sidewall opening type; ——, covered ridge with sidewall opening type; - - - -, Nääs et al. (1998)

the CRSP type. Values of E for the CRSP type ranged from 0·90 to 1·00, 0·68 to 0·90 and 0·47 to 0·62 at wind speeds of 1·5, 3 and 4·5 m s^{-1}, respectively, for a roof slope of 10–30°.

In comparing the SP and CRSP results with that of Nääs *et al.* (1998) (*Fig. 6*), the values of E for the SP type was lower than that for the CRSP type when the roof slope was under 30°, but vice versa when the roof slope was greater than 30° at wind speeds of 5 and 10 m s^{-1}. Values of E for both type are less than that obtained by Nääs *et al.* (1998). *Fig. 6* also shows that the values for E changed smoothly with roof slope when roof slope was $>30°$.

The equations and charts presented, allow for the calculation of opening effectiveness for wind-induced natural ventilation in traditional agricultural buildings of Taiwan. Estimates of opening effectiveness in a scale model can be obtained through wind tunnel experiments. A wide range of operating conditions must be applied to the wind tunnel experiments, to allow the evaluation of average opening effectiveness by means of dimensionless equations. This may prove difficult in commercial buildings, unless they are monitored over the entire season.

5. Conclusions

Opening effectiveness in sidewall opening type and covered ridge with sidewall opening type was observed under different wind speeds, ratios of height to length of opening, wind angles of incidence, and roof slopes. An algorithm of opening effectiveness using different parameters was derived from dimensional analysis and scale model study in a wind tunnel test.

Wind speed and wind angle of incidence were the dominant factors affecting opening effectiveness in both sidewall openings and covered ridge with sidewall openings. Opening effectiveness increased with increasing wind angle of incidence up to 90°. It also increased with increasing ratio of height to length of opening, especially increasing rapidly when the ratio was $<1/6$. The larger roof slope resulted in lower opening effectiveness, but the variations become smooth when roof slope was larger than 30°. All experiments showed that higher wind speed resulted in lower opening effectiveness for both types.

To favour wind-induced natural ventilated openings, the opening should face the prevailing wind direction, cutting the ratio of height to length of opening to at least 1/6, whilst higher ratios are preferred. The roof slope should be as flat as possible. The comparison of opening effectiveness E between the side wall opening type and the covered ridge with sidewall opening type shows insignificance for the wind-induced natural ventilation system at specific wind speeds of 5 and 10 m s^{-1}. If buoyancy is considered, the covered ridge with sidewall opening type may conduct ventilation with both wind-induced and buoyancy forces beneficially.

The opening effectiveness of the prototype enclosures can be predicted by the results of the scale model experiments in a wind tunnel as the appropriate similitude criteria were applied. Further study need to test non-isothermal conditions to realistic represented enclosures. Validation of the opening effectiveness from scale model study in predicting prototype behaviour is needed. The efficiency of natural ventilation enclosures using combined wind-induced and buoyancy forces also needed to be evaluated.

References

Albright L D (1976). Airflow through hinged baffle slotted inlets. Transactions of the ASAE, **19**(4), 728–732, 735

Albright L D (1990). Environment Control for Animals and Plants. ASAE Publishing, St Joseph, MI, USA

ASHRAE (1997). Handbook of Fundamentals. American Society of Heating, Refrigerating and Air Conditioning Engineers, Inc., Atlanta, GA. USA

Aynsley R M (1988). A resistance approach to estimating airflow through buildings with large openings due to wind. ASHRAE Transactions, **94,** 1661–1668

Barrington S; Zemanchik N; Choiniere Y (1994). Orienting livestock shelters to optimize natural summer ventilation. Transactions of the ASAE, **37**(1), 251–255

Choiniére Y (1991). Wind induced natural ventilation of low-rise building for livestock housing by the pressure difference method and concentration decay method. PhD Thesis, University of Ottawa

de Jong T; Bot G P A (1992). Air exchange caused by wind effects through (window) openings distributed evenly on a quasi-infinite surface. Energy and Buildings, **19**(2), 93–103

de Zwart H F; Bot G P A (1997). Energy saving prospectives of combined heat and power in horticulture in the Netherlands: a simulation study. Netherlands Journal of Agricultural Sciences, **45**(1), 97–107

Esmay M L; Dixon J E (1986). Environmental Control for Agricultural Buildings. AVI Publishing Co, Inc., Westport, CT, USA

Fox R W; McDonald A T (1973). Introduction to Fluid Mechanics. John Wiley & Sons, Inc., New York, NY

Hellickson M A; Hinkle C N; Jedele D G (1983). Natural ventilation. In: Ventilation of Agricultural Structures (Hellickson MA; Walker JM, eds), pp. 81–100 ASAE Publishing, St. Joseph, MI, USA,

Liao C M; Chiu K H (2002). Wind tunnel modeling the system performance of alternative evaporative cooling pads in Taiwan region. Building and Environment, **37**(2), 177–187.

Miguel A F; van de Braak N J; Silva A M; Bot G P A (1998). Physical modeling of natural ventilation through screens and windows in greenhouses. Journal of Agricultural Engineering Research, **69**(2), 133–139

Miguel A F; van de Braak N J; Silva A M; Bot G P A (2001). Wind-induced airflow through permeable materials Part II: air infiltration in enclosures. Journal of Wind Engineering and Industrial Aerodynamics, **89**(1), 59–72

Murphy G (1950). Similitude in Engineering. The Ronald Press Co., New York, NY

Nääs I A; Moura D J; Bucklin D A; Fialho F B (1998). An algorithm for determining opening effectiveness in natural ventilation by wind. Transactions of the ASAE, **41**(3), 767–771

Shepherd D G (1965). Elements of Fluid Mechanics. Brace & World, Harcourt, New York, NY

Verlinde W; Gabriels D; Christiaens J P A (1998). Ventilation coefficient for wind-induced natural ventilation in cattle buildings: a scale model study in a wind tunnel. Transactions of the ASAE, **41**(3), 783–788

Young D F (1994). Similitude, Modeling, and Dimensional Analysis in Engineering. Unpublished Lecture Notes and Problems for Em584 in Iowa State University.